

## Size-affected shear-band speed in bulk metallic glasses

Z. Y. Liu, Y. Yang, and C. T. Liu

Citation: *Appl. Phys. Lett.* **99**, 171904 (2011); doi: 10.1063/1.3656016

View online: <http://dx.doi.org/10.1063/1.3656016>

View Table of Contents: <http://apl.aip.org/resource/1/APPLAB/v99/i17>

Published by the [American Institute of Physics](http://www.aip.org).

---

### Related Articles

Nonlinear viscoelasticity of freestanding and polymer-anchored vertically aligned carbon nanotube foams  
*J. Appl. Phys.* **111**, 074314 (2012)

Defect-induced solid state amorphization of molecular crystals  
*J. Appl. Phys.* **111**, 073505 (2012)

Notable internal thermal effect on the yielding of metallic glasses  
*Appl. Phys. Lett.* **100**, 141904 (2012)

Sheared polymer glass and the question of mechanical rejuvenation  
*J. Chem. Phys.* **136**, 124907 (2012)

Growth stress in SiO<sub>2</sub> during oxidation of SiC fibers  
*J. Appl. Phys.* **111**, 063527 (2012)

---

### Additional information on *Appl. Phys. Lett.*

Journal Homepage: <http://apl.aip.org/>

Journal Information: [http://apl.aip.org/about/about\\_the\\_journal](http://apl.aip.org/about/about_the_journal)

Top downloads: [http://apl.aip.org/features/most\\_downloaded](http://apl.aip.org/features/most_downloaded)

Information for Authors: <http://apl.aip.org/authors>

## ADVERTISEMENT



**PFEIFFER**  **VACUUM**

Complete Dry Vacuum Pump Station  
for only **\$4995** — HiCube™ Eco

800-248-8254 | [www.pfeiffer-vacuum.com](http://www.pfeiffer-vacuum.com)

## Size-affected shear-band speed in bulk metallic glasses

Z. Y. Liu,<sup>1</sup> Y. Yang,<sup>1,a)</sup> and C. T. Liu<sup>2,a)</sup>

<sup>1</sup>Department of Mechanical Engineering, The Hong Kong Polytechnic University, Hung Hom, Kowloon, Hong Kong

<sup>2</sup>Department of Mechanical and Biomedical Engineering, Centre for Advanced Structural Materials, City University of Hong Kong, Tat Chee Avenue, Kowloon, Hong Kong

(Received 18 July 2011; accepted 4 October 2011; published online 24 October 2011)

In this letter, we report an important experimental finding and theoretical analysis of the shear-band speed measured in a variety of bulk metallic-glasses. Unlike the prior work, in which the shear-band speed was regarded as a constant, our current study, based on carefully designed loading-holding cyclic tests, reveals that the speed of a shear band correlates with its resultant shear offset. Such a correlation arises as a “size” effect, which could be rationalized with the energy balance principle and shear-banding dynamics entailing initial shear softening and subsequent materials recovery. © 2011 American Institute of Physics. [doi:10.1063/1.3656016]

Plasticity in bulk metallic glasses (BMGs) is well known to be shear-band (SB) mediated at room temperature (RT), which manifests as localized plastic flows confined into a banded region with a nano-scale thickness.<sup>1</sup> Unlike dislocation-mediated plasticity in crystalline materials, the RT plasticity in BMGs generally exhibits a “size effect,”<sup>2–6</sup> i.e., SBs tend to propagate catastrophically if unhindered, causing brittle-like fracture in large samples; while they tend to propagate in a “stick-slip” manner in small samples, leading to serrated plastic flows.

Over the past decades, considerable efforts have been devoted to understanding the plasticity and the related size effect in BMGs,<sup>1–6</sup> among which one outstanding issue is the speed of a mature SB. In the literature, measurements of the SB speed have been attempted by different means, such as cinematography,<sup>7,8</sup> strain gauge,<sup>9</sup> and acoustic signal detection,<sup>10,11</sup> but seemingly contradictory results, ranging from  $\sim 10 \mu\text{m s}^{-1}$  to  $\sim 1 \text{m s}^{-1}$ , have been reported up to date. Unlike the speed of dislocation movement in crystals, the measurable speed of shear-banding in BMGs should be attached to a simultaneous shearing process, which causes shear-offset formation along a pre-established shear plane under compression.<sup>5–7,11</sup> Since it is already known that the magnitude of a shear offset is size dependent in BMGs,<sup>5</sup> it is hence natural to raise the question whether such size dependence still persists in the SB speed. However, in the prior work, the measurement of a SB speed was performed for a particular size of shear offset,<sup>8,9,12</sup> and there still lacks a systematic investigation of the size dependence of SB speed in BMGs. In the present work, we intend to address this question using the microcompression approach to measure the SB speed at different shear offsets.

To conduct microcompression experiments, the focused-ion-beam (FIB) sequential milling approach<sup>4,13</sup> was utilized to fabricate micropillars on the surfaces of a variety of BMGs, including Zr-, Ti-, Fe-, Mg-, and Cu-based BMGs (see supplemental material for their chemical composi-

tions<sup>21</sup>). Before the FIB treatment, the BMGs were checked using x-ray diffraction to ensure their amorphous structure (not shown here) and then mechanically polished to a mirror finish on their surfaces. The details of the FIB milling have been described elsewhere<sup>4,13</sup> and a total of 31 micropillars was fabricated on the BMG samples with the diameter and aspect ratio ranging from  $\sim 1$  to  $\sim 2 \mu\text{m}$  and 2:1 to 4:1, respectively. Afterwards, microcompression experiments were conducted on the modified Hysitron<sup>TM</sup> nanoindentation system, which has the resolution of  $\sim 1 \text{nm}$  in displacement and  $\sim 1 \mu\text{N}$  in load and was then equipped with a  $10\text{-}\mu\text{m}$  flat-end diamond punch.

Unlike the previous microcompression experiments,<sup>12</sup> the load function we adopted here is composed of multiple “loading-holding” cyclic tests, as shown in Fig. 1(a). The experimental set-up came out of an inspiration gained from the recent findings of anelasticity in BMGs,<sup>14–16</sup> which implies that yielding in BMGs may result from the percolation of local anelasticity events. If that was so, yielding might be triggered by a time-dependent process at an appropriate stress level. To facilitate data collection, the holding load was programmed to start from  $\sim 80\%$  of the estimated quasi-static yielding load and then increased by  $\sim 5\%$  per cycle. It should be noted that the loading rate was varied from  $5 \times 10^2 \mu\text{N/s}$  to  $1 \times 10^5 \mu\text{N/s}$  in an effort to assess the possible loading-rate effect on pop-in, as discussed in Ref. 17, while both the holding and unloading time were set at  $\sim 2 \text{s}$ , which suffice to relax anelastic deformation in the micropillars according to the previous findings.<sup>14</sup> As such, the remaining deformation during the holding time, if there were still any, should result from the local plasticity events in the micropillars.

Figure 1(a) shows a whole time-displacement curve corresponding to the load spectrum designed. As seen, the micropillar deforms initially in an apparent elastic manner, which is validated by the full recovery of the micropillar deformation after unloading. However, with the increasing load, yielding finally occurs, causing displacement burst or pop-in. Within our expectation, these pop-in events took place mainly during the holding periods, as clearly seen in Figs. 2(b)–2(d). After the finish of the test, it was found that

<sup>a)</sup>Authors to whom correspondence should be addressed. Electronic addresses: mmyyang@polyu.edu.hk (Tel.: 852-2766-6652) and chainliu@cityu.edu.hk (Tel.: 852-3442-7213).

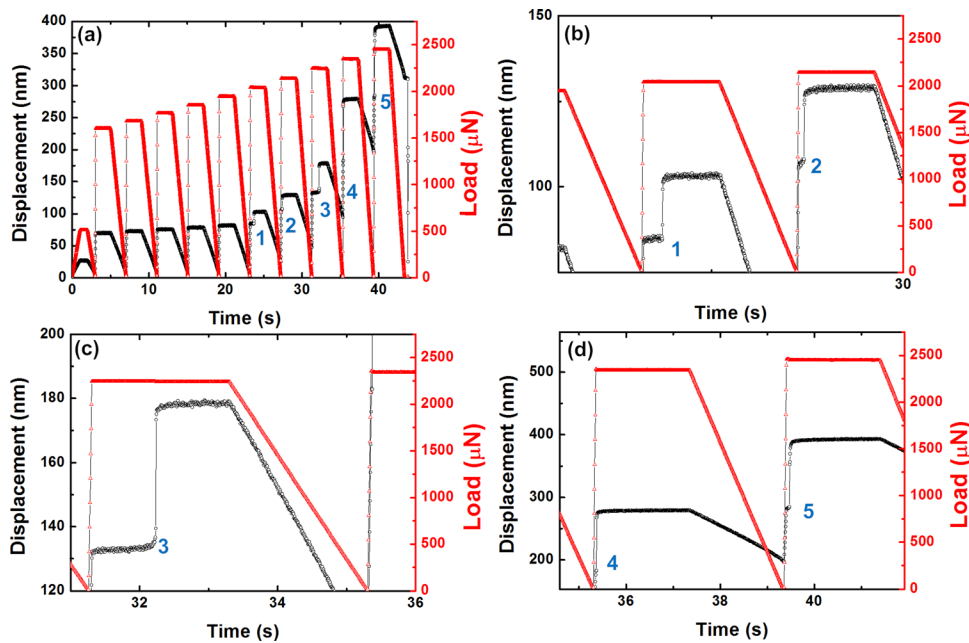


FIG. 1. (Color online) (a) The overall time-displacement displacement curve (black) displaying five pop-in events triggered at five consecutive holding periods (as indicated by the numbers) and the corresponding load spectrum programmed for the microcompression experiment; (b) to (d) the enlarged views of the five pop-in events.

the number of pop-in was in good agreement with that of the SBs observed on the micropillar. The experimental observations indicate that each pop-in event corresponds to one SB operation in the micropillar. Furthermore, it is worth pointing out that the loading rate was found to play little role in determining the size of the pop-in occurring during holding,

which validates our experiments as a size-effect study in which the possible rate effect has been ruled out.

As a highlight, Fig. 2(a) presents the details of the load and displacement versus time data, which characterize the pop-in event occurring during holding. Similar to the previous observations,<sup>8,9</sup> the SB seemingly experienced four stages of propagation, i.e., acceleration, sliding, deceleration, and final arrest in the deformed micropillar. However, attention should be drawn to the well-maintained load constancy. Even at the instant of pop-in, the applied load only drops by  $\sim 5 \mu\text{N}$ , which is negligibly small and only counts up to  $\sim 0.2\%$  of the programmed holding load. Following the method of Song *et al.*,<sup>8</sup> the displacement rate,  $\dot{h}$ , which corresponds to the stage of viscous gliding as shown in Fig. 2(b), was used to calculate the SB speed,  $V$ , for a given displacement jump  $\Delta h$ . Assuming the shear angle  $\theta \sim 45^\circ$  [Fig. 2(c)], one can obtain the SB speed and the corresponding shear offset  $s$  as  $V = \dot{h} / \cos \theta$  and  $s = \Delta h / \cos \theta$ , respectively. Figure 3 presents the results of the SB speed so obtained as a function of  $s$  from different BMGs. Regardless

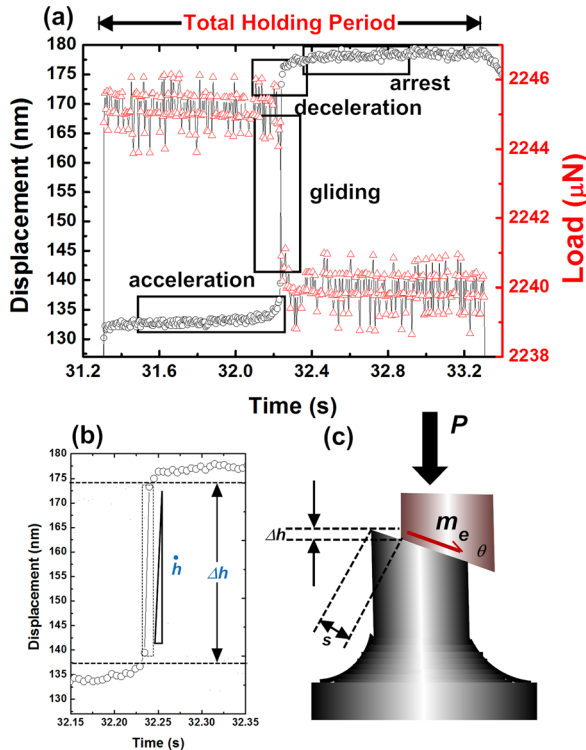


FIG. 2. (Color online) (a) The enlarged view of the discontinuities in the collected mechanical signals featuring a delayed pop-in event triggered in the holding period; (b) the portion of the time-displacement curve used to measure the displacement jump  $\Delta h$  and the corresponding characteristic displacement speed,  $\dot{h}$ , for the pop-in event; and (c) the sketch illustrating that the displacement-jump forms as the upper part of the micropillar glides along the inclined shear plane with the lower part of the micropillar remaining rest.

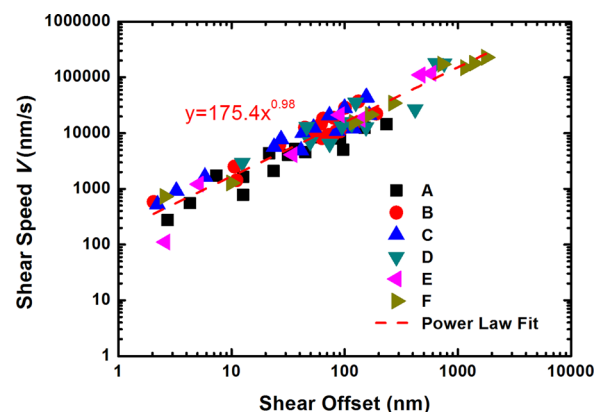


FIG. 3. (Color online) The double logarithmic plot of the measured shear speed versus shear offset for six types of BMGs with A =  $\text{Zr}_{55}\text{Pd}_{10}\text{Cu}_{20}\text{Ni}_5\text{Al}_{10}$ , B =  $\text{Cu}_{46.25}\text{Zr}_{44.25}\text{Al}_{7.5}\text{Er}_2$ , C =  $\text{Ti}_{40}\text{Zr}_{25}\text{Ni}_3\text{Cu}_{12}\text{Be}_{20}$ , D =  $\text{Zr}_{55}\text{Cu}_{28}\text{Ni}_5\text{Al}_{10}\text{Nb}_2$ , E =  $(\text{Fe}_{44.3}\text{Cr}_5\text{Co}_5\text{Mo}_{12.8}\text{Mn}_{11.2}\text{B}_{5.9})_{98.5}\text{Y}_{1.5}$ , and F =  $\text{Mg}_{58}\text{Cu}_{31}\text{Nd}_5\text{Y}_6$ .

of their chemical compositions, the measured SB speeds clearly exhibit a “size” effect, i.e., the larger is the shear offset the higher is the SB speed and seemingly follow a same trend that can be fitted by a power law. Nevertheless, it is worth mentioning that fitting the individual trend of the size effect obtained for different BMGs reveals a possible material dependence in the size-effect phenomenon, the details of which, however, have exceeded the scope of the current investigation and will be studied as our future work (see supplementary material for the fitting of the individual trend of the size effect<sup>21</sup>).

To rationalize the observed size effect, let us turn to the kinetics of shear-banding in BMGs. At any instant of SB propagation, the energy balance should be maintained irrespective of the BMGs chemical composition, which can be expressed in a rate form as  $\dot{W} = \dot{U}_e + \dot{K} + \dot{D}$ , where  $W$ ,  $U_e$ ,  $K$ , and  $D$  denote the work done by an external agent, the elastic energy storage, the kinetic energy, and the plastic energy dissipation, respectively, and the over-dot represents the time derivative of a physical quantity. For our microcompression experiments, in which the shear band propagates at a holding load, it can be deduced that  $\dot{W} = Ph = \tau_0 A_s V_s$ , where  $\tau_0$  is the initial shear stress,  $V_s$  the instantaneous shear speed, and  $A_s$  the area of the shear plane;  $K = 1/2 m_e V_s^2$ , where  $m_e$  is the effective mass of the micropillar moving along with the shear band and  $D = A_s \int \tau(t) V_s dt$ , where  $\tau(t)$  denotes the instantaneous shear strength remaining on the shear plane. Note that owing to the limited shear offset as compared to the pillar’s diameter, any change in  $A_s$  due to the SB propagation is neglected here for simplicity. Combining the above equations, one can derive the following formula for the instantaneous shear speed  $V_s$ :

$$V_s(t) = \frac{A_s}{m_e} \left\{ \int_0^t [\tau_0 - \tau(t)] dt - \frac{1}{A_s} \int_0^t \frac{dU_e}{ds} dt \right\}. \quad (1)$$

Based on the prior work,<sup>5,18</sup> it is known that BMGs experience initial shear softening and subsequent recovery in a shear-banding event. Theoretically, such a physical picture of shear-banding dynamics can be inferred from Eq. (1). When shear softening dominates the material behavior, the elastic energy stored in the vicinity of the shear band is released ( $dU_e/ds < 0$ ), which is accompanied by the increase of  $V_s$ ; however, at the later stage of recovery, the elastic energy storage is regained ( $dU_e/ds > 0$ ) with the material hardening and diminishing shear speed. To obtain the maximum shear speed, one can solve  $\dot{V}_s(t) = 0$  for the critical time,  $t_c$ , and substitute  $t_c$  into Eq. (1) to derive its full speed  $V = V_s(t_c)$ . In our experiments, the shear speed measured from the stage of viscous gliding is an experimental approximation of  $V_s(t_c)$ .

To shed light on the cause of the size effect, Eq. (1) needs to be transformed. After the necessary mathematic arrangements (see supplementary material for details<sup>21</sup>), one could reach a simple relation,  $V = \sqrt{C_1 \Delta u_e + C_2 \Delta \Gamma}$ , where  $C_1$  and  $C_2$  are two material dependent constants;  $\Delta u_e$  is the volumetric density of the elastic energy released up to the time  $t_c$ , and

$\Delta \Gamma$  can be understood as a normalized complementary energy dissipation and proportional to  $\int_0^{s_c} [\tau_0 - \tau(s)] ds$  with  $s_c$  denoting the shear displacement at  $t_c$ . Given such a relation, the size effect on the shear speed can be explained as a manifestation of the known size dependence of the elastic energy release,  $\Delta u_e$ , in BMGs, i.e., the larger is a shear offset the more is the normalized elastic energy released upon shear banding. The cause of the size effect on  $\Delta u_e$  has been discussed thoroughly in the literature<sup>2,5,6,19</sup> and can be generally ascribed to the dimensional misfit between the three-dimensional elastic energy release and two-dimensional plastic energy dissipation during shear-banding in BMGs. Apart from that, it is obvious that the complementary energy dissipation  $\Delta \Gamma$  also contributes to the size effect at constant loading. However, in conventional tests with load serrations, the applied load drops with  $\tau(t)$ , which tends to nullify the effect of  $\Delta \Gamma$ .

In summary, the dependence of the SB speed on the shear offset in BMGs is uncovered in this study. Due to the generality of energy balance, it appears universal for the physical origin of this emerging size effect as compared with those of many other similar phenomena already found for BMGs, such as the sample size effect on malleability,<sup>2,5</sup> shear offsets,<sup>20</sup> and thermal profile around a SB.<sup>6</sup>

Y.Y. acknowledges the financial support provided by the Research Grant Council (RGC), the Hong Kong Government, through the General Research Fund (GRF) with the account No. PolyU 5359/09E.

<sup>1</sup>Y. Zhang and A. L. Greer, *Appl. Phys. Lett.* **89**(7), 071907 (2006).

<sup>2</sup>Y. Yang, J. C. Ye, J. Lu, P. K. Liaw, and C. T. Liu, *Appl. Phys. Lett.* **96**(1), 011905 (2010).

<sup>3</sup>H. Guo, P. F. Yan, Y. B. Wang, J. Tan, Z. F. Zhang, M. L. Sui, and E. Ma, *Nature Mater.* **6**, 735 (2007).

<sup>4</sup>C. A. Volkert, A. Donohue, and F. Spaepen, *J. Appl. Phys.* **103**(8), 083539 (2008).

<sup>5</sup>J. C. Ye, J. Lu, Y. Yang, and P. K. Liaw, *Acta Mater.* **57**, 6037 (2009).

<sup>6</sup>Y. Q. Cheng, Z. Han, Y. Li, and E. Ma, *Phys. Rev. B* **80**(13), 134115 (2009).

<sup>7</sup>S. X. Song, H. Bei, J. Wadsworth, and T. G. Nieh, *Intermetallics* **16**(6), 813 (2008).

<sup>8</sup>S. X. Song, X. L. Wang, and T. G. Nieh, *Scr. Mater.* **62**(11), 847 (2010).

<sup>9</sup>W. J. Wright, M. W. Samale, T. C. Hufnagel, M. M. LeBlanc, and J. N. Florando, *Acta Mater.* **57**(16), 4639 (2009).

<sup>10</sup>F. H. Dalla Torre, D. Klaumünzer, R. Maaß, and J. F. Löffler, *Acta Mater.* **58**(10), 3742 (2010).

<sup>11</sup>A. Vinogradov, *Scr. Mater.* **63**(1), 89 (2010).

<sup>12</sup>H. M. Chen, J. C. Huang, S. X. Song, T. G. Nieh, and J. S. C. Jang, *Appl. Phys. Lett.* **94**(14), 141914 (2009).

<sup>13</sup>Y. Yang, J. C. Ye, J. Lu, F. X. Liu, and P. K. Liaw, *Acta Mater.* **57**, 1613 (2009).

<sup>14</sup>J. C. Ye, J. Lu, C. T. Liu, Q. Wang, and Y. Yang, *Nature Mater.* **9**(8), 619 (2010).

<sup>15</sup>Y. H. Liu, D. Wang, K. Nakajima, W. Zhang, A. Hirata, T. Nishi, A. Inoue, and M. W. Chen, *Phys. Rev. Lett.* **106**, 125504 (2011).

<sup>16</sup>W. Dmowski, T. Iwashita, C.-P. Chuang, J. Almer, and T. Egami, *Phys. Rev. Lett.* **105**, 205502 (2010).

<sup>17</sup>C. A. Schuh, A. C. Lund, and T. G. Nieh, *Acta Mater.* **52**, 5879 (2004).

<sup>18</sup>S. X. Song and T. G. Nieh, *Intermetallics* **17**(9), 762 (2009).

<sup>19</sup>Y. Yang, J. C. Ye, J. Lu, Y. F. Gao, and P. K. Liaw, *JOM* **62**(2), 93 (2010).

<sup>20</sup>F. F. Wu, Z. F. Zhang, and S. X. Mao, *Acta Mater.* **57**, 257 (2009).

<sup>21</sup>See supplementary material at <http://dx.doi.org/10.1063/1.3656016> for their chemical compositions and the fitting of the individual trend of the size effect.